11th IGTC
Dispatchable technology & innovations for a carbon-neutral society
10-11 October 2023, Brussels, Belgium
Paper ID Number: 9-IGTC23

VALIDATION OF A LIFING APPROACH FOR A DIGITAL FLEET OF GAS TURBINES

A. J. Moffat*, Solar Turbines Inc., R. Green, Solar Turbines Inc.,
C. Meyer, Solar Turbines Inc., J. Maxted, Frazer-Nash Consultancy

329 Doncastle Road, Bracknell, UK
+44 1344 782924
*Moffat_andrew_j@solarturbines.com

ABSTRACT

Gas turbines are being increasingly stretched to operate more flexibly, outside of their original product design requirements, due to changes in the commercial, regulatory and legislative environment. This poses a challenge for the lifing of industrial gas turbines as more flexible operation results in more complex loading.

OEMs and operators have developed lifing strategies and tools that can account for this flexible operation. OEMs have developed design methodologies and created service offerings that can allow operators to work their engines harder or extend the time between overhauls. These methodologies have matured into tools that use a range of data sources and modelling techniques to predict component life. Physics based models, combined with operational data, are required so that life beyond original product design requirements can be predicted accurately.

This paper presents a lifing approach that has been embedded within our digital twin fleet to predict the initiation of material damage. The approach enables the prediction of a material response for each component based on its operational history.

This paper demonstrates how the lifing approach has been validated using notched bar tests, which are representative of the geometry of critical locations in a gas turbine. The paper also contains details about how the lifing approach has been validated using ex-service components.

INTRODUCTION

Industrial gas turbines (IGTs) are operated in ways that are increasingly varied. On one side of the spectrum, they are operated as base load, or continuous duty (i.e. long periods of operation at constant load, with few shutdowns), whilst at the other side of the spectrum they are operated for emergency duty applications or peak shaving applications (i.e. frequent short duration cycles). Within the spectrum of operation are varying environments and fuels that add complexity to understanding the remaining useful life of a specific turbine.

There are three key drivers for the increasingly flexible operation of IGTs, these are legislation, regulations and customer demand. In Europe regulations, such as Grid Code, requires IGTs to remain connected to the grid even if the grid frequency drops. Each country has its own interpretation of the code, resulting in different time periods and power requirements. For single shaft power generation IGTs to comply with these new rules, the turbine must increase firing temperature as the frequency drops in order to generate more power and provide the needed stability the regulation is intended to address. Depending on application, this could require the IGT to increase firing temperature above the standard ratings for short periods of time until the grid stabilizes. With regard to customer expectation, there are a number of requirements such as service flexibility, turbine life extension and sanctioned increases in firing temperature above the standard rating for short durations to meet peak power requirements, (i.e. on hot days when ambient conditions limit power output).

This demand for flexible operation creates unique challenges for existing IGTs, particularly with regard to critical life limited components (Zhou et al. 2021). These components may have been designed with different requirements and need to be re-evaluated to keep up with the changing environment and expectations. Traditional redesign approaches may not be ideal in this rapidly evolving market. OEMs and operators are therefore continuing to develop lifing strategies and tools that can account for this flexible operation. Advances in computing provides high quality data that can be exploited to understand the conditions of assets more accurately (Green et al., 2018). This has enabled OEMs to develop approaches that can allow operators to optimize their equipment for an expanded range of applications.

Data analytics provides a route to the prediction of a state of a component based on previous experience. But to provide confidence in predictions outside of the usual operating envelope, physics-based models are required. Material models are a core part of the physics that must be captured. Previous papers have demonstrated how the

material response can be predicted under complex loading behaviour (Moffat et al., 2020 and Green et al., 2016) in standard test samples used for LCF. These material models need to be implemented into a wider lifing strategy to predict the state of more complex samples and real components. OEMs and other industries have developed multiple different lifing strategies. In this work the lifing strategy has been based on the British R5 nuclear assessment code (Ainsworth 2006 and 2014). The approach in R5 is well validated, having been used to life ageing nuclear plant for decades.

The lifing approach presented in this paper enables the prediction of a material state (quantity of damage) for each component based on its operational history. In this paper it is demonstrated how the lifing approach has been used to predict the life of notched bar tests. These tests are more reflective of the geometry of critical locations in a gas turbine. It is also demonstrated how the lifing approach can be used to understand the state of real components and how this supports flexible operation.

The paper will provide a brief overview of the lifing strategy used in this work. Material models are a key input into the lifing calculations and a brief description of them is provided. Notched bar tests were undertaken to validate the lifing strategy and the paper details the experimental methods, finite element analysis undertaken to support the testing, and results of these tests. The damage calculations for the notched bar tests are provided and similar calculations for a component for a sub-fleet of engines is presented. The paper concludes with a section on the wider implications of this work for gas turbines and the services this approach enables to substantiate the flexible operation of IGTs.

LIFING STRATEGY

The authors have implemented a lifing approach that allows high value components in an IGT fleet to be individually lifed. The life of each component is based on its operational history and measurements from the engine. This is converted to a material response and ultimately used to predict the state of damage (remaining life) in the component.

With unlimited computing power it would be possible to develop performance, thermal and structural models for an individual engine in a fleet. However, this is not yet possible and so an approach is required that reduces the scale of the problem to a one-dimensional calculation that can be undertaken at a number of key locations in a component. These reduced order models are a key component of the lifing approach for a fleet of engines.

An underlying performance model must be developed for each engine type (or configuration). This performance model enables different cycles to be developed that span the typical performance space of an IGT. The performance cycles model typical transients as well as full load conditions. Thermal models are developed for each performance cycle. A structural FE model is developed for the 'normal operation' cycle and this cycle is used to identify bounding locations on components. This process is described in more detail in (Green et al. 2019 and Scaletta et al., 2020). Once critical locations are determined, thermal and structural reduced order models (ROMs) are developed. The ROMs are fitted on several engine cycles and validated on others to ensure they provide an accurate response for a wide range of operating conditions and to check they can extrapolate sensibly. Software codes such as Ansys provide access to ROM methods.

A key feature of the ROMs is that they link measured engine parameters (temperature, pressure, speed) to metal temperature and stresses at the key locations using physics based equations. When the ROMs are combined with measured data for an IGT it is possible to calculate the stresses and temperatures specific to a location in an engine. It should be noted that the stress ROMs are fitted to linear elastic stresses. This is done for computational reasons; it is typically much easier to develop linear-elastic models for complicated engine assemblies. The R5 cycle construction approach is used with the Neuber method and the suite of material models to calculate the material response at a location and track the state of the material over the life of the component.

A key feature of the R5 (Ainsworth, 2006 and 2014) lifing method is that the initiation of a crack is defined as the point at which the combined creep and fatigue damage equals 100%. This differs to the ASME method of specific damage interaction plots for individual or groups of materials (Spindler, 2007). The coverage of the ASME creep-fatigue interaction plots is limited for the alloys of primary interest to IGTs and so the R5 approach is more robust for the range of Nickel and other alloys in an IGT.

Bounding assumptions are used for stress, material properties and temperature in design assessments to provide a deterministic bounding assessment of damage (or life). But the assessment of multiple gas turbines in-service is a probabilistic problem. A probabilistic framework has been developed (Cathcart e al., 2020) which uses input distributions to obtain a probabilised output. This output can be used to make risk based decisions.

This lifing strategy and supporting models have been embedded in a lifing tool. The tool is connected to a database containing operational data for a fleet of gas turbines. An example of the results from this tool is presented later in the paper.

MATERIAL MODELS

In some senses the R5 method is relatively simple. It allows creep damage and fatigue damage to be calculated separately and uses linear summation of damage to calculate the state of the material. However, the approach also accounts for creep-fatigue interaction. This is achieved through detailed modelling of the material (stress-strain) response and this is often where complexity arises. The lifing approach requires a suite of material models to enable

both the material response and damage to be predicted. These include:

- Creep deformation
- Plastic deformation
- Physical properties
- Tensile properties
- Creep damage
- Fatigue damage

Creep Deformation

The form of the creep deformation model is not defined in R5. In previous papers (Moffat et al., 2014 and 2020) the authors have demonstrated how different forms of creep models can be used to accurately describe both the constant load and constant strain response of materials. This is particularly important in real components where both primary loads (pressure and CF) and secondary loads (thermal) are present.

Gas turbine components seldom fail due to tertiary creep as they are designed to avoid the high primary loads that can cause this. So, the creep model must be most accurate in the primary and secondary creep regimes. In previous work (Moffat et al., 2020) the authors presented the development of a backstress model for creep, based on the Lemaitre-Chaboche (1994 and 2008) viscoplasticity model. The form of this model allows both primary and secondary creep to be modelled. One of the attractions of the backstress approach is that it is based on micro-mechanistic observations. Several authors, for example Al Mamum et al. (2015) and Peng et al., (1988) have measured the evolution of internal stress and demonstrated the link between the internal stress and dislocation movement. The backstress model is therefore a convenient and, importantly, an implementable solution to represent the micro-mechanistic behaviour of a material through global parameters.

In Moffat et al. (2020) it was shown that a backstress model predicted the primary-secondary response of a typical creep curve well and could also account for changes in stress during a dwell. The creep deformation model was validated using the creep response during dwells in strain-controlled fatigue-dwell tests at various conditions.

Plastic Deformation

Again, the form of the plastic deformation model is not specified in R5. In the work presented in this paper a conventional Ramberg-Osgood model has been used to predict cyclic plasticity. This model does not capture the effect of strain rate or isotropic behaviour on the plastic response like a Lemaitre-Chaboche type model. However, it is a reasonable approach for practical application. From a materials perspective, Ni-based allows tend to reach cyclic stability reasonably quickly as isotropic hardening is not significant after the first few cycles. Also. the loading rate does not vary significantly in components, therefore strain rate effects are not particularly significant.

A Lemaitre-Chaboche type model could provide benefit to potentially unify creep and plasticity into a single inelastic deformation model. But the cost of material data to develop such an approach, for multiple materials, along with the difficulty implementing it means that this has not been pursued in this work. It is also worth considering the computation cost of implementing more complex models. This can severely limit the ability to provide near-real time predictions when a gas turbine fleet is large.

Physical and Tensile Properties

Standard, temperature dependent models have been used for physical and tensile properties and so no further details are provided in this paper on these models. The physical properties are used both in the Finite Element analysis presented later in this paper and in the construction of the materials response for lifing calculations (with modulus and Poisson's ratio being required to model the elastic response of the material).

Creep Damage

The lifing method in this work uses the ductility exhaustion approach to calculate creep damage. This is consistent with the R5 method. The ductility exhaustion approach is detailed in literature (Spindler, 2007; Holdsworth, 2019; Skelton and Gandy, 2008) and the authors have previously presented their model in Green et al. (2016).

The basic premise of the ductility exhaustion approach is that a material can withstand a certain amount of inelastic strain, and once that limit is reached a crack is considered to have initiated. The basic form of the damage (d_{in}) model for the ductility exhaustion approach is:

$$d_{in} = \int_0^t \frac{\dot{\varepsilon}_{in}}{\varepsilon_f(\dot{\varepsilon}_{in}, T)}\, dt \qquad (1)$$

where $\dot{\varepsilon}_{in}$ is the inelastic strain rate and $\varepsilon_f(\dot{\varepsilon}_{in}, T)$ is the ductility which is dependent on temperature (T). The model was derived using standard constant load creep tests as discussed in Green et al. (2016). At low strain rates, typical of those experienced in long creep tests at low stress, a materials ductility tends to be lower than at high creep strain rates, for example in high stress creep rupture tests. As discussed in Skelton and Gandy (2008) this is due to different damage mechanisms occurring at different combinations of stress and temperature (Smith et al., 2016).

An alternative to ductility exhaustion is an estimation of damage based on time to creep rupture. Both time to rupture and ductility at failure are recorded in a creep test and so both approaches are valid ways of measuring damage. However, whilst time to rupture is convenient to measure it does not explicitly describe the state of the material. It is beyond the scope of this paper to compare the two approaches (see Spindler (2007) for an example of this comparison). However, ductility exhaustion was chosen in this work due to the satisfactory results obtained with it

(demonstrated later in the paper) and the more physical nature of the model compared to the time based rupture approach.

Fatigue Damage

Fatigue damage is calculated using Miner's rule. This approach is simple and consistent with most assessment codes (including ASME, RCC-MR in addition to R5). The underlying fatigue endurance model is not prescribed in these codes. There are two key considerations when fitting a fatigue model for an automated lifing approach: 1) it must represent both the low and high cycle regimes well so it is generally applicable and 2) it must be temperature dependent to avoid interpolation between test temperatures.

An example of a fatigue endurance model was discussed in Green et al., (2019) and is reproduced in Figure 1. The model used in this work is proprietary, but it is based on a Langer (1962) model with temperature dependent material parameters. A Walker (1970) mean stress correction is also applied to account for the effect of R-ratio. As can be seen in Figure 1, there is scatter in the material's data. In the lifing method this is accounted for using a probabilistic framework (Cathcart et al., 2019 and 2020). Each of the material models, not just fatigue, has a probabilistic distribution that is accounted for in the lifing method.

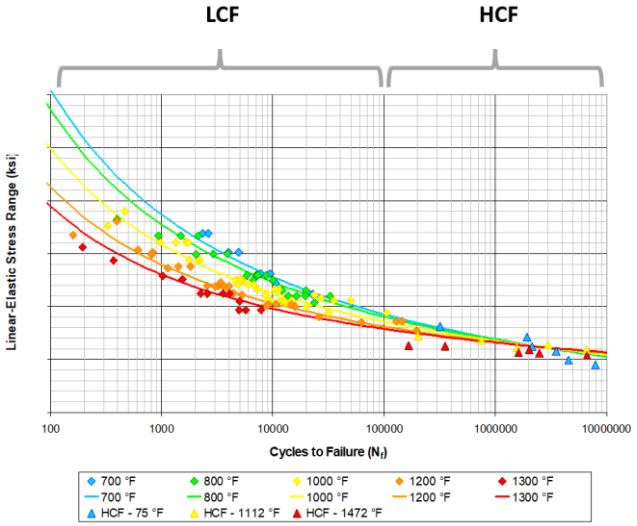

FIGURE 1: FATIGUE ENDURANCE MODEL AFTER (Green et al., 2019)

EXPERIMENTAL METHODS

Fatigue dwell tests were performed on notched bars to support the validation of the lifing approach, and material models, on complex geometries. The material that has been investigated in this study is IN718, which is a precipitation hardened superalloy. IN718 contains a high quantity of Cr and so exhibits good corrosion resistance. IN718 is typically used for components that operate up to a temperature of 700°C. Whilst IN718 exhibits good creep resistance up to this temperature, creep deformation must be considered at the upper end of the operating envelop when considering structural integrity.

Load controlled fatigue and fatigue-dwell testing of the notched bar samples was in accordance with ASTM E466 and ASTM E2714. Specimens with stress concentration factors (Kt) of 2.4, 3.7 and 4.5 were evaluated. An example of the Kt=2.4 notched bars is provided Figure 2. The fatigue tests employed a triangular waveform at 20 cycles per minute. In the fatigue-dwell tests a 15, 30 or 60 minute (constant strain) dwell was applied at the peak tensile strain in each cycle. The tests were conducted at temperatures between 510°C and 620°C. A total of thirteen fatigue-dwell and ten fatigue tests (from the same cast for comparison) were undertaken. The global R-ratio of the tests was a value of 0.

The strain at the center of the notch is difficult to measure without using techniques such as Digital Image Correlation (DIC). However, global strain across the notch was measured using a clip gauge.

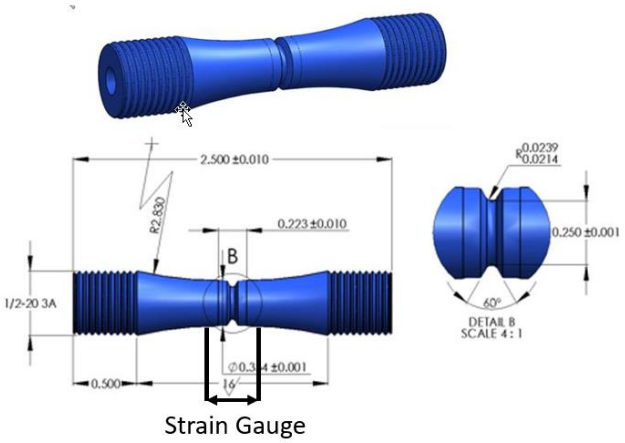

FIGURE 2: GEOMETRY FOR A NOTCHED BAR STRESS CONCENTRATION FACTOR OF 2.4. MEASUREMENTS ARE IN INCHES

EXPERIMENTAL RESULTS

The notched bar fatigue test results are presented in Figure 3. The net section stress ranges have been normalized relative to the highest stress test. It can be seen in Figure 3 that the data collapse onto each other when the net section stress is multiplied by the Kt value. The Kt=2.4 tests were at a lower temperature but there is not much effect of temperature on fatigue over this temperature range (see Figure 1).

Lives of approximately 500 to 2000 cycles were targeted for the tests. The stresses are somewhat higher than might be expected in a typical engine. Fatigue-dwell tests were conducted at 510°C and 538°C. The lives of the fatigue dwell tests have been compared with the relevant fatigue (no dwell) tests in Figure 4. It can be seen in Figure 4 that the fatigue dwell tests have lower lives than the fatigue tests. The detriment in life is due to the additional creep damage

in the fatigue-dwell tests. The tests at 510°C exhibited a smaller reduction in life than the tests at 538°C. This is expected because less creep damage should occur at the lower temperature. The reduction in life due to fatigue in the 538°C tests is approximately a factor of 4.

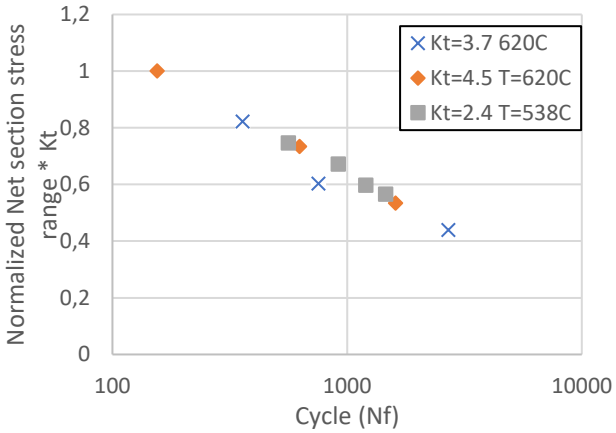

FIGURE 3: NOTCHED BAR FATIGUE RESULTS WITH STRESS NORMALIZED

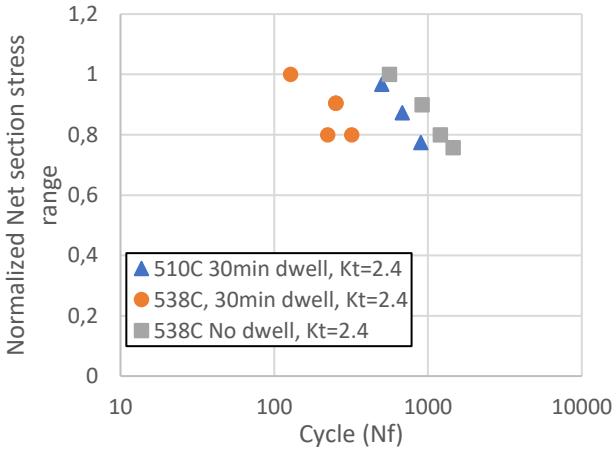

FIGURE 4: CYCLES TO FAILURE FOR THE KT=2.4 NOTCHED BAR TESTS

Macrograph images comparing the fracture surfaces of a fatigue specimen (A) and a fatigue-dwell specimen (B) are presented in Figure 5. Initiation on the fatigue specimen occurred at multiple locations around the circumference of the notch and propagated uniformly toward the centre until ductile overload failure occurred. Initiation on the fatigue-dwell specimen also occurred at multiple locations around the notch circumference but propagated non-uniformly, as indicated by the heat tinted area. The notch surface of the fatigue-dwell specimen exhibited more inelastic deformation than the notch surface of the fatigue specimen. The initiation sites in the fatigue dwell samples tended to be transgranular in appearance (see Figure 6) but grew in an intergranular manner. In the fatigue specimen the initiation region and crack growth region both appeared to be intergranular.

The cycles to failure for the higher temperature Kt=3.7 and Kt=4.5 specimens are presented in Figure 7. There is a significant reduction in life in the fatigue-dwell samples due to creep. The Kt=4.5 tests have lower lives than the Kt=3.7 tests as might be expected (for the same net section stress). The stresses in these tests are high and the lives are well below the target of 500 to 2000 cycles. The peak stresses in the notches are beyond the validity range of the fatigue and creep models discussed in Material Models section above. Therefore, only the lower stress tests in Figure 7 (at a normalized stress of 0.73 and 0.53) were used in the Damage Predictions presented later in this paper.

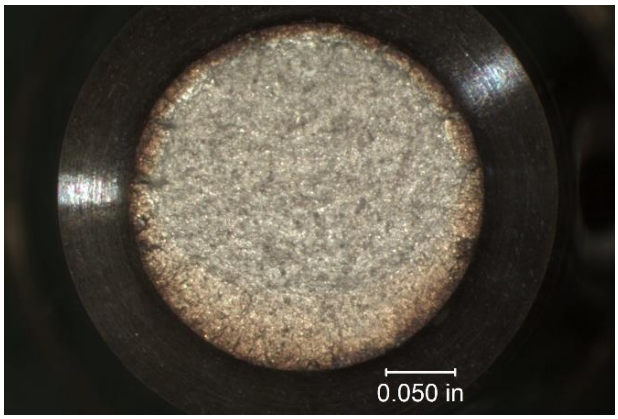

(A)

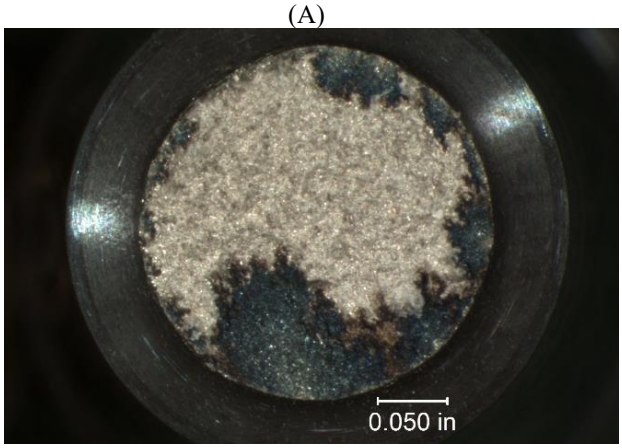

(B)

FIGURE 5: MACROGRAPHS OF TYPICAL FRACTURE SURFACES FOR KT=2.4 SAMPLES AT 538°C, (A) IS A FATIGUE SAMPLE AND (B) IS A FATIGUE-DWELL SAMPLE.

FINITE ELEMENT ANALYSIS

Finite element (FE) analysis was undertaken for three reasons:

- Linear elastic FE analysis to confirm the stress concentration factors for the different specimens were calculated correctly.

- Linear elastic FE analysis as an input into the lifing tools to predict specimen damage and life.
- Elastic-plastic analysis to enable a comparison of the material response in the notch between finite element theory and the lifing tool.

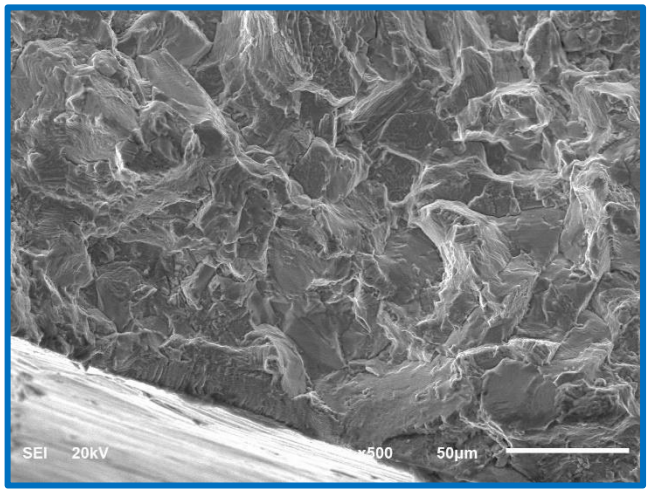

FIGURE 6: AN INITIATION SITE IN A FATIGUE-DWELL SPECIMEN.

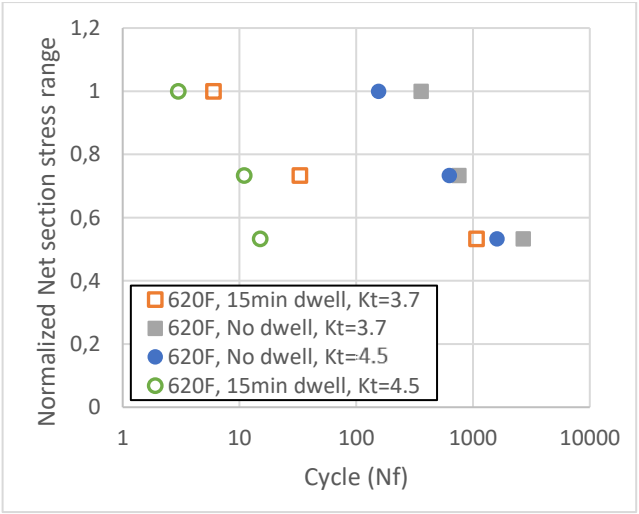

FIGURE 7: CYCLES TO FAILURE FOR THE KT=3.7 AND KT=4.5 NOTCHED BAR TESTS.

Linear Elastic FE Analysis

FE analysis was undertaken in Ansys. A 3-dimensional solid body model with SOLID186 elements were used, the mesh is shown Figure 8 for a Kt of 3.7. The mesh was highly refined around the notch. The model was fixed at one end to limit displacement in the axial direction. However, the bar was not constrained in the radial and circumferential directions. A pressure was applied to the other end of the model in order to load the sample.

For the calculation of stress concentration factors, the values estimated using the Kt value and net section stress were within 1% of the linear elastic stress in the FE model results. It was concluded that the design of the different notched bar samples was accurate.

Linear Elastic to Elastic-Plastic Stress in the Lifing Tool

The lifing tool uses linear elastic stresses as an input. The elastic-plastic material response is calculated in the lifing tool using a Ramberg-Osgood model and the Neuber method. The linear-elastic FE model was used to create a cycle response input for the peak stress location in each test that could be processed in the lifing tool. The lifing tool material response for one of the fatigue tests is presented in Figure 9. After a ¼ cycle of significant plasticity, the lifing tool predicts a stable cycle. The mean stress relaxes over the first few cycles so that the material response at that location has an R-ratio of -1, despite the global R-ratio being 0. This is a consistent trend for all the fatigue tests and so the others are not shown here.

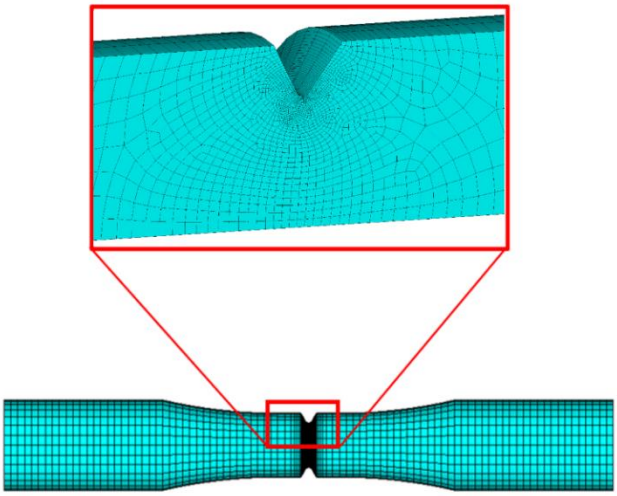

FIGURE 8: EXAMPLE MESH FOR THE FE ANALYSIS OF THE KT=3.7 NOTCHED BAR

Elastic-Plastic FE Analysis

An elastic-plastic FE model was run to verify the elastic-plastic material response of the lifing tool. As discussed previously, a Ramberg-Osgood plasticity model is used in the lifing tool. This Ramberg-Osgood model was implemented in Ansys. The material response for the first cycle, for one of the fatigue tests, is presented in Figure 9 for comparison with the response from lifing tool. It can be seen that the initial loading response of the FEA provides more plasticity than the lifing tool. But the stabilized cycles are approximately similar in appearance. The lifing tool cycles exhibit a slightly larger strain range than the FEA. Nevertheless, the comparison shows that the use of linear-elastic stresses in the lifing tool, and the supporting methods and material models, provides a reasonable approximation

of the material response when compared with the elastic plastic FE.

Creep FE Analysis

The creep response for a dwell during one of the fatigue-dwell tests is presented in Figure 10 for comparison with the response from lifing tool. The development of creep strain over the dwell is approximately similar. This provides confidence that the creep deformation model is correctly implemented in the lifing tool. The small difference in the behaviour is well within the experimental and material uncertainty which is accounted for in the probabilistic framework (Cathcart et al., 2019 and 2020) used in the lifing tool.

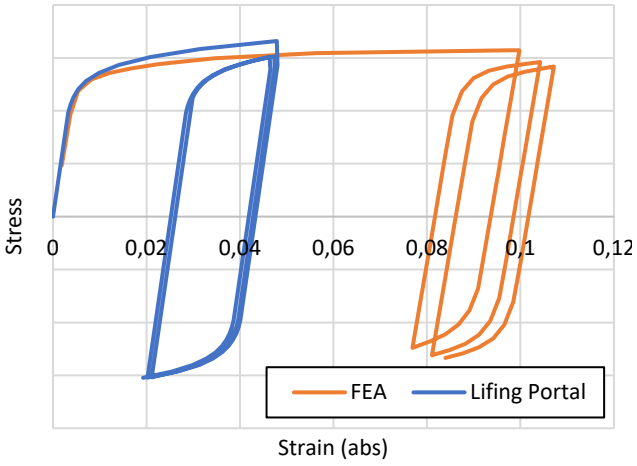

FIGURE 9: COMPARISON OF THE ELASTIC-PLASTIC MATERIAL RESPONSE CALCULATED IN THE LIFING TOOL AND FE MODEL FOR A TEST

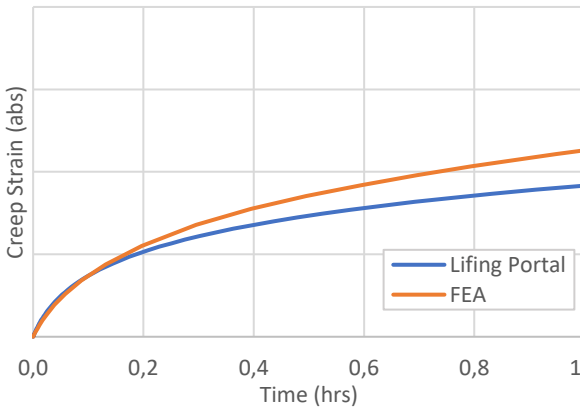

FIGURE 10: COMPARISON OF CREEP STRAIN DURING A DWELL IN THE FE ANALYSIS AND THE LIFING TOOL

DAMAGE PREDICTIONS FOR NOTCHED BARS

The notched bar experiments provide a route to validate the lifing approach and tools. The geometry is not as complicated as a typical IGT component. However, many critical locations in IGT components are at fillets and notches and so a notched bar is broadly representative. The lifing approach has been applied to the notched bars. A linear-elastic FE model was analysed using the location selection method (Green et al., 2019, Scaletta and Green, 2020) to identify the key location that limits the life of the specimen. For an isotropic material that is the centre of the notch. Thermal and Stress ROMs were developed. The step that converts engine data to stresses and temperatures, for engine components, was not required for the test samples. The lifing tool was used to calculate the fatigue and creep damage for each test. The damages were combined using the R5 linear summation approach to predict damage.

It is convenient to present the creep and fatigue damage values on a single plot (one damage mechanism on each axis); the damage plot for the notched bar tests is presented in Figure 11. The axes are usually presented on a log scale (Spindler, 2007) as both creep and fatigue tend to have log normal distributions. The fatigue tests have zero creep damage, but they are presented as having a small creep damage (0.1%) so that they can be seen in Figure 11.

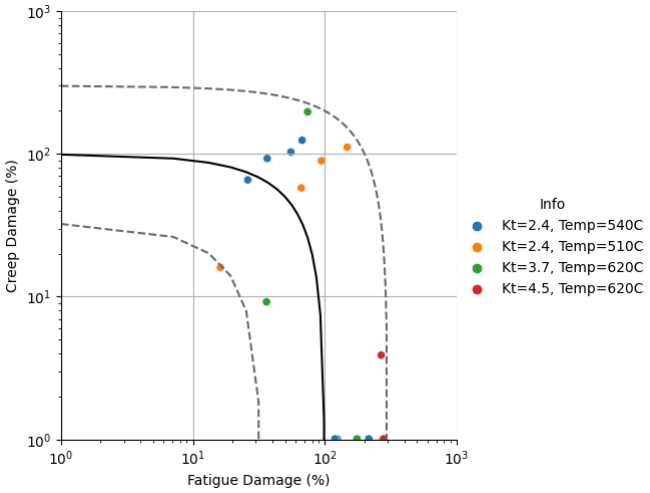

FIGURE 11: DAMAGE PLOT FOR THE DIFFERENT NOTCHED BAR TESTS

The solid black line in Figure 11 represents 100% damage. At every point along the line the sum of the creep and fatigue damage equals 100%. The dashed line represents a factor of 3 on the damage value. It is worth noting that in low cycle fatigue data the uncertainty on life is often a factor or 2 or 3 and so these bounds represent the typical uncertainty that might be expected for these tests. If the lifing approach and underlying material model were perfect, and there was no material or test uncertainty, then the data points would sit on the 100% damage line. Data points lying above and to the right of the 100% damage line

indicate the damage has been over predicted (and therefore the life of the specimen is under-predicted); this is a conservative prediction. Data points below and to the left of the 100% line indicate an under-prediction of the damage which is non-conservative.

In reality there are uncertainties in the tests and assumptions in the lifing method and so some scatter in the results would be expected. For a best estimate prediction there should be a similar number of data points either side of the 100% line. It can be seen in Figure 11 that there are some points either side of the line but that the majority of tests were conservatively predicted. From a practical engineering point of view, some conservatism in a best estimate prediction is acceptable, OEMs do not want components to initiate cracks. But it does indicate there are conservative assumptions in the method that can be explored further (for example the inclusion of notch sensitivity in the calculation of fatigue and creep damage – see below). The data points are generally within the level of expected scatter and so it is concluded that the lifing approach predicts the notched bar tests well. These results provide good validation of the lifing tool.

It can be seen in Figure 11 that the fatigue damage is over-predicted in the fatigue samples. They tend to be clustered around a damage of 200%. The fatigue model is based on smooth sided specimens (Moffat et al. 2020). It is likely that the conservative prediction of damage is due to the absence of a notch strength correction method in the underlying lifing approach. This will be the subject of future work for both isotropic and anisotropic materials.

The creep damages in the fatigue dwell tests are clustered around a value of 100%. It is expected that they should be a little lower (as they also have a fatigue damage component). Again, this might be a notch strength effect that needs further investigation. However, the results indicate that the creep deformation model and ductility exhaustion approach provide representative damages.

DAMAGE PREDICTIONS FOR A COMPONENT

The creep model was presented and verified against smooth sided, strain-controlled, fatigue dwell tests in Moffat et al. (2020). The wider lifing approach, has been validated on notched bar specimens in the previous section. The lifing methods and models have been coded into the lifing tool and have been used to calculate the state of real components in a fleet of IGTs. A case study for a component is presented in this section.

The lifing tool is proprietary and so can't be presented. Besides containing the lifing methods it also contains engine data. It is the combination of the lifing approach and engine data that results in a digital twin of an engine. A collection of digital twins can be described as a digital fleet, which represents the physical fleet. So the lifing tool houses the digital fleet.

These creep and fatigue damage values have been extracted from the lifing tool for a single component in a subset of similar engines and presented in Figure 12. Some of the components were at the end of service (orange points) and the others were in-service but approaching the end. It can be seen that all the damages are well away from the 100% and lower bound lines indicating that initiation of a crack should not have occurred in these components (although with the statistical nature of lifing methods this cannot always be guaranteed). There is quite a variation in the damage values and this is based on how each individual engine has been operated. It can be seen in Figure 12 that this component tends to be creep dominated with creep damages up to 20% in some engines. Only three engines have fatigue damages greater than 1%.

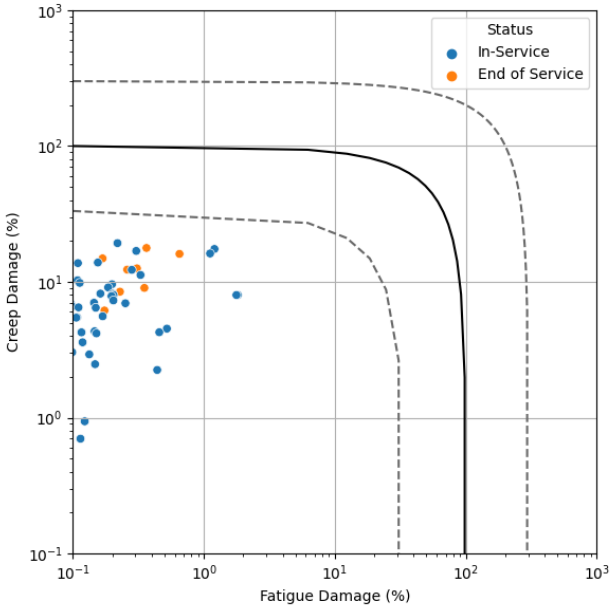

FIGURE 12: DAMAGE PLOT FOR A COMPONENT

A number of the end of service components have been inspected. Microstructural changes associated with creep were observed. It is not possible to quantify the damage in the components based on observations to confirm the values in the damage plot. However, based on the qualitative assessment the observations and predictions appear to be consistent.

With a firm understanding of the state of a component it is possible to make decisions about extending the life of a component or operating an engine more flexibly. For example this component has more life that could be utilised. This would exploit the gap between the design and the real state of the components. The services that have been developed to allow these decisions are discussed in the next section. But it is important to remember that these services are based on a firm physical understanding of the stresses, temperature, and material behaviour in IGT components.

IMPLICATIONS FOR GAS TURBINES

The energy transition is creating unique challenges for IGTs, especially for legacy equipment which may have been

designed several decades earlier with very different requirements. Legacy engines cannot simply be replaced to accommodate these continuous changes. Firstly, the transition is still underway and as such the future requirements are not yet defined, (i.e. fuel specifications for hydrogen). And secondly, the costs would be prohibitive and the time scales impractical. Therefore, it is imperative that existing energy infrastructure and equipment be managed through this transition.

It is incumbent upon OEMs to support this transition by determining the suitability of existing equipment to respond to the demands of the market and the needs of customers. Ensuring the safe and effective operation of equipment, under increasingly flexible requirements, is paramount. Technologies that are developed to manage IGTs must be capable of modelling and quantifying the impact of increased firing temperature or extending service periods.

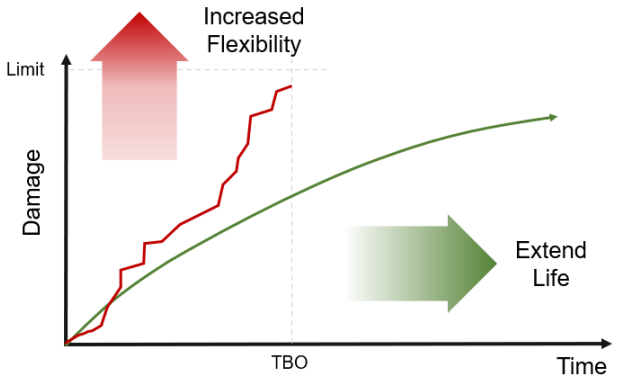

FIGURE 13: TYPICAL REQUIREMENTS FOR AN IGT

Digital twins are one technology that can be employed to assist asset management and optimization of IGTs (Green et al, 2018). Digital twins must be capable of accurately predicting the durability of engine components in a reasonable timeframe. Material models that predict key damage mechanics, such as creep and fatigue are therefore critical to the effectivity of digital twins. Without well validated material models incorporated in a validated lifing approach, damage accumulation predictions, and therefore durability, may be inaccurate. This would severely limit the use of digital twins to manage the required flexibility in operation.

A digital twin that is able to account for an increase in firing temperature on the damage accumulation of IGT components could be used to manage IGTs safely and effectively throughout the service period. Using a digital twin it is possible to provide a durability status throughout an engine's operation; this is the red line shown schematically in Figure 13. The red line illustrates how periods of low and high load can be balanced out to achieve the Time Between Overhaul (TBO) within the damage limit. Similarly, the same digital twin could be used to extend the life of an engine safely and effectively beyond typical service periods under the right conditions, i.e. low load applications; this is shown schematically by the green line in Figure 13.

Solar Turbines Incorporated have expanded the range of equipment health management (EHM) services through the *InSight Platform* ® supported by digital twin technology. *Power Boost*^{TM} is an OEM sanctioned product available with EHM service, providing owner/operators the option to temporarily increase firing temperature to exceed rated power capability. This type of flexible operation provides additional power on hot days, during emergency duty applications, or when it's valuable to provide additional, temporary power to driven equipment. These capabilities can support the reduction of CO_2 by avoiding oversizing equipment for a power requirement at a high ambient temperature that may only occur for a few hours a year, or by minimizing spinning reserve and allowing a running unit to increase its power output to compensate for a tripped unit. The same approach can be applied to managing the impact of grid instability for single shaft engines or extending operation of a unit beyond the traditional TBO, optimizing schedule and cost. Digital twins are a key technology to support the energy transition but require the ability to predict durability accurately and effectively under a range of operating conditions.

CONCLUSIONS

OEMs and operators of IGTs continue to develop lifing approaches and tools to support the increasingly flexible operation of IGTs. It is essential to understand, and be able to model, the underlying material response of materials to support flexible operation.

A lifing approach was validated using notched bar tests with different values of stress concentration factor. The life of the samples is predicted well. There is a slight over-prediction in damage, which is conservative, but this is considered to be acceptable. Further work is required to determine if a notch strength correction is required in the lifing approach to increase accuracy.

A case study of an IGT component demonstrates how the lifing approach has been implemented in a lifing tool; this is a key technology in the digital twin of an engine.

Individual assessments of damage for IGTs in a fleet of engines were presented. The variation in damage due to the different operation of the engines was demonstrated. The assessments in the lifing tool enable services that support the flexible operation of IGTs. These tools exploit the gap between design assumptions and the way individual engines are operated to support flexible operation.

The purpose of this lifing approach is the accurate prediction of the durability and life of engine components. Future work will concentrate on the validation of these approaches both with feature tests and ex-service components.

ACKNOWLEDGEMENTS

The authors would like to acknowledge the support of Dr. Richard Bellows at Solar Turbines Incorporated.

REFERENCES

Ainsworth, R.A., R5 Procedures for Assessing Structural Integrity of Components under Creep and Creep-Fatigue Conditions, International Materials Reviews, Volume 51, no 2, pp 107-126, 2006.

Ainsworth, R. A., Hales, R., Budden, P. J., Martin, D. C, (eds), Assessment Procedure for the High Temperature Response of Structures. Nuclear Electric Rep. R5, Issue 3, Revision 2, 2014.

Al Mamun, A., Moat, R.J., Bouchard, P.J., Origin and Effect of Backstress on Cyclic Creep Deformation of 316H Stainless Steel, Proceedings of the ASME PVP Conference, PVP 2015-4552, July, 2015, Boston, MA, USA.

Cathcart, H., Horne, G., Parkinson, J., Moffat, A. and Joyce, M., Probabilistic Methods: Risk Based Design and Assessment, Proceeding of the ASME PVP 2019, PVP2019-93557, July 2019, San Antonio, Texas, USA.

Cathcart, H., Meyer, C., Joyce, M. and Green, R., Probabilistic Lifing Methods for Digital Assets, Proceedings of ASME Turbo Expo 2020, June 2020, London, UK.

Chaboche, J.L., A Review of Some Plasticity and Viscoplasticity Constitutive Theories, International Journal of Plasticity, Volume 24, 1642-1693, 2008.

Green, R.J. and Douglas, J.P., Impact of Engine Operation on Gas Turbine Component Durability using Ductility Exhaustion, The Future of Gas Turbine Technology 8th International Gas Turbine Conference, 12th-13th October 2016, Brussels, Belgium.

Green, R., Douglas, J., Moffat, A., Bellows, R., Characterizing the Influence of Cyclic Re-Priming on the Prediction of Long Term Creep Damage for Gas Turbine Components, Proceedings of ASME Turbo Expo 2018, June 2018, Oslo, Norway.

Green, R., Allen, C., Fox, B., Holcomb, C. and Leon, M., Overview of Digital Asset Management for Industrial Gas Turbine Applications, 9th International Gas Turbine Conference, October 2018, Brussels, Belgium.

Green, R., Moffat, A., Douglas, J. and Scaletta, B., An Approach to Identify Bounding Damage Locations for Condition Based Structural Integrity Assessments of Gas Turbine Components, Proceedings of ASME Turbo Expo 2019, GT2019-91894, June 2019, Phoenix, Arizona, USA.

Holdsworth, S., Creep-Ductility of High Temperature Steels: A Review, Metals, Volume 9, Issue 3, pp. 342, 2019

Langer, B., Design of Pressure Vessels for Low-Cycle Fatigue, ASME Journal of Basic Engineering, Volume 84 pp. 389-402, 1962

Lemaitre, J., Chaboche J.-L., Mechanics of Solid Materials, Cambridge University Press, 1994, ISBN 0 521 47758 1.

Moffat, A.J., Douglas, J.P., White, M., Spindler M.W., Austin, C., and Jaques, S., Development of the RCC-MR Creep Deformation Model for the Prediction of Creep and Stress Relaxation in Type 321 Stainless Steel, Proceeding of the ASME PVP 2014, Orange County, CA, USA.

Moffat, A., Green, R., Ferguson, C. and Scaletta, B., Development of a Constitutive Backstress Model for the Prediction of Creep and Stress Relaxation in Gas Turbine Materials, Proceedings of ASME Turbo Expo 2020, June 2020, London, UK.

Peng, X., Zeng, X. and Fan, J., A Physically Based Description for Coupled Plasticity and Creep Deformation, Int. J. Solids Structures, Vol. 35, No. 21, pp2733-2747, 1988.

Scaletta, B. and Green, R., Critical Location Identification for Multi-mechanistic Damage Modes Using Damage Interaction Charts, Proceedings of ASME Turbo Expo 2020, June 2020, London, UK.

Skelton, R.P. and Gandy, D., Creep – fatigue damage accumulation and interaction diagram based on metallographic interpretation of mechanisms, Materials at High Temperatures, Volume 25, Issue 1, 2008

Smith, T.M., Unocic, R.R., Deutchman, H. and Mills, M.J., Creep Deformation Mechanism Mapping in Nickel Based Superalloys, Materials and High Temperature, Volume 33, Issue 4-5, Pages 373-383, 2016.

Spindler, M.W., An Improved Method for the Calculation of Creep Damage During Creep-Fatigue Cycling, Materials Science and Technology, Volume 23, Issue 12, pp. 1461-1470, 2007.

Walker, K. The effect of stress ratio during crack propagation and fatigue for 2024-T3 And 7075-T6 aluminum. In Effects of Environment and Complex Load History on Fatigue Life; ASTM International: West Conshohocken, PA, USA, 1970.

Wilshire, B. and Battenbough, A.J., Creep and Creep Fracture of Polycrystalline Copper, Materials Science and Engineering: A, Volume 443, Issues 1-2, pp. 156-166, 2007.